Scaling of Horizontal Convection at High Rayleigh Number

Tzekih Tsai[1*], Martin P. King[2] and Gregory J. Sheard[1]

[1]The Sheard Lab, Department of Mechanical and Aerospace Engineering, Monash University

[2]Uni Research, and Bjerknes Centre for Climate Research, Norway

*tzekih.tsai@monash.edu

1. INTRODUCTION

Horizontal convection describes convection flow driven in an enclosure by non-uniform heating imposed across a horizontal boundary [1], and serves as an idealised model for global ocean currents. These flows are characterised by a Rayleigh number Ra representing the strength of buoyancy over dissipative effects, and a Prandtl number *Pr* representing the ratio of molecular to thermal dissipation in the fluid. Overturning flow exists at all Rayleigh numbers, while higher Rayleigh numbers invoke a convective regime characterised by thin thermal and kinematic boundary layers adjacent to the forcing boundary that scale inversely with Nusselt number *Nu* [2] characterising the horizontal heat transport. The scaling of Nusselt number with Rayleigh number is critical to our understanding of the role of buoyancy destabilisation in driving global ocean currents. In horizontal convection, Nusselt number is based on the net vertical heat flux over the thermal forcing boundary.

Rossby [2] developed scaling for forcing boundary layer quantities in thermal convection heated unevenly from below. Assuming a balance between vertical thermal diffusion into the thermal boundary layer from the base and horizontal transport of heat within the boundary layer leads to scaling of boundary layer thickness as $h \sim Ra^{-1/5}$ and Nusselt number as $Nu \sim Ra^{1/5}$.

These flows were known to become unsteady beyond some Rayleigh number, Sheard *et. al.* [3] reported unsteady flow beyond $Ra = 6 \pm 2.5 \times 10^8$. The effect of unsteady flow on horizontal convection scaling was first recognised by Sheard *et. al.* [3], where simulations across several enclosure height ratios demonstrated *Nu–Ra* scaling exponents exceeding *1/5*. Theoretical support for higher power-law exponents in the scaling for Nu is availed by the variational analysis of Siggers [4], which places an upper bound of *1/3* on the scaling exponent. This study aims to resolve the apparent shift in the scaling exponent at high Rayleigh numbers

2. METHODOLOGY

The system comprises a rectangular enclosure of width L and height H filled with an incompressible fluid where a Boussinesq model for buoyancy is employed. All boundaries are rigid and impermeable, satisfying the no-slip condition $u = 0$. Adiabatic boundary conditions are imposed on side and top boundaries, while along the forcing boundary a linear temperature profile is imposed ranging from $\theta = 0$ at $(x, y) = (0,0)$ to $\theta = 1$ at $(x, y) = (1,0)$. The incompressible Boussinesq Navier-Stokes equations are solved using a nodal spectral element method for spatial discretisation and a third-order operator-splitting scheme based on backwards-differentiation for time integration.

Numerical simulations are performed with an aspect ratio $H/L = 0.16$, and a Prandtl number $Pr = 6.14$, representative of water, due to the motivating interest in global ocean circulation. The domain is discretised into a conforming grid of 12500 quadrilateral spectral elements with polynomial degree ranging from 4 at lower Ra up to 6 for a $Ra = 3.2 \times 10^{13}$. Elements are clustered towards the bottom forcing boundary and the hot end of the enclosure to capture the

boundary layers, plumes and any unstable flow dynamics. All simulations are time-evolved to a statistically steady state before time-averaged Nusselt numbers are calculated.

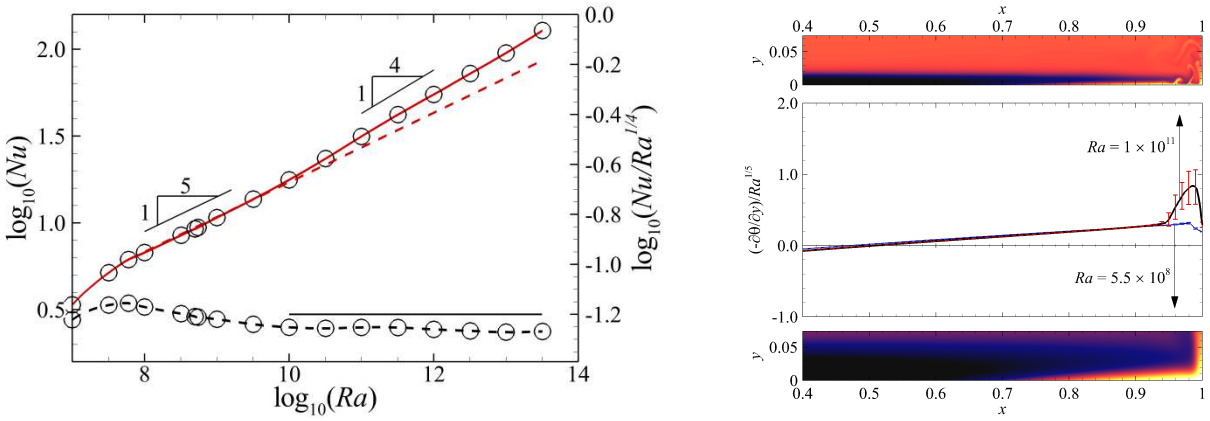

(a) *(b)*

Figure 1. (a) A plot of $\log_{10}Nu$ (red solid line) and $\log_{10}(Nu/Ra^{1/4})$ (black dashed line) against $\log_{10}Ra$. Two triangles of $1/5$ and $1/4$ gradient are included for guidance, the red dashed line is a projected $1/5$ scaling extended from $Ra = 3.2 \times 10^9$. (b) A plot of $-(\partial\theta/\partial y)/Ra^{1/5}$ against x over the hotter 60% of the forcing boundary. Solid lines show the time mean data, and error bars the standard deviation. Instantaneous temperature fields are included above and below the plot.

3. RESULTS

The dependence of Nusselt number on Rayleigh number is shown in Figure 1(a). The convective regime establishes beyond $Ra = 3.2 \times 10^7$, adopting Rossby's $Ra^{1/5}$ scaling. The $Ra^{1/5}$ scaling holds through the time-periodic regime, but the onset of the irregular flow regime brings an elevated scaling for Nusselt number going with $Ra^{0.24\pm0.01}$. This regime is robust, adhering close to $Ra^{1/4}$ for more than four decades in Rayleigh number.

A physical understanding of this $Ra^{1/4}$ regime is aided by consideration of the vertical thermal gradient, $\partial\theta/\partial y$, along the forcing boundary. Where Rossby's $Ra^{1/5}$ scaling holds, $\partial\theta/\partial y$ at different Rayleigh numbers should coincide when scaled by $Ra^{1/5}$. Figure 1(b) compares two cases: a case ($Ra = 5.5 \times 10^8$) exhibiting to the $Ra^{1/5}$ scaling in Figure 1(a), and a case ($Ra = 10^{11}$) exhibiting $Ra^{1/4}$ scaling. Along much of the forcing boundary, the normalised thermal gradients are coincident. Beyond $x \approx 0.94$, the higher-Ra case exhibits a significant increase in thermal gradient. This in turn increases Nusselt number beyond Rossby's $Ra^{1/5}$ scaling. The elevated thermal gradients are produced across the hottest part of the base where unsteady flow features manifest in the form of buoyant mushroom plumes ascending from the forcing boundary upstream of the end-wall (compare the instantaneous thermal fields in Figure 1(b)).

4. CONCLUSIONS

High-order spectral-element simulations identify a $Nu \sim Ra^{1/4}$ scaling regime in horizontal convection at high Rayleigh number. This reveals that the horizontal convection model plays a more important role in the ocean heat transport budget.

REFERENCES

[1] Hughes, G. O., & Griffiths, R. W. (2008) Horizontal convection. *Annu. Rev. Fluid Mech.*, **40**, 185-208.

[2] Rossby, H. T. (1965) On thermal convection driven by non-uniform heating from below: an experimental study. *Deep Sea Research and Oceanographic Abstracts*, **12**, 9-16.

[3] Sheard, G. J., & King, M. P. (2011) Horizontal convection: Effect of aspect ratio on Rayleigh number scaling and stability. *Applied Mathematical Modelling*, **35**(4), 1647-1655.

[4] Siggers, J. H., Kerswell, R. R., & Balmforth, N. J. (2004) Bounds on horizontal convection. *J. Fluid Mech.*, **517**, 55-70.